## 1. Circuit Analysis with Time Varying Passives

→ most sensors appear as a time varying passives

→ Many of them change so slowly, they can be considered as time-invariant

ex: humidity sensor

→ But some change so quickly that they must be considered as time-variant

ex: displacement sensor in a MEMS resonator

∴ How do we perform circuit analysis with time-variant passives?

### a. Time-variant resistors

ex: piezoresistive displacement sensor

Consider a Thevenin equivalent DC circuit with DC sources and resistors only (op amps ok)

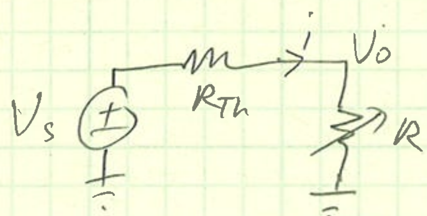


ex: $R = R_0 + R_a \sin(\omega t)$ where $R_0 > R_a$

$$V_o = V_s \frac{R}{R+R_{Th}} = \frac{V_s(R_0 + R_a \sin(\omega t))}{R + R_0 + R_a \sin(\omega t)}$$

→ closed form solution

→ nonlinear result → one frequency in, multiple frequencies out

## b. Time-variant Reactive Elements

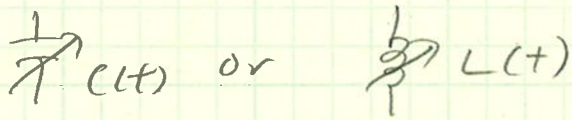


Circuit assumptions:

1. DC sources only
2. no other reactive elements
3. resistor and op amp networks

→ Form thévenin equivalent circuit for C(t) or Norton equivalent circuit for L(t)

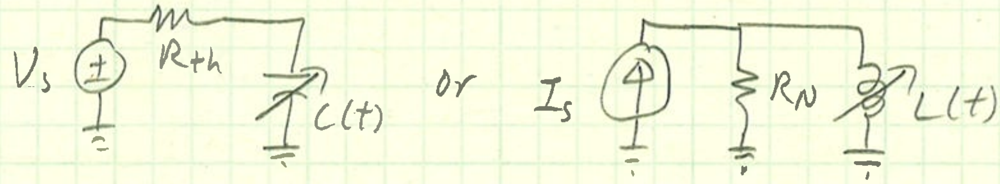


→ For time-variant reactive devices:

$i_C(t) = \dot{C}V_c + \dot{V}_c C$ and $V_L(t) = L\dot{i}_L + i_L\dot{L}$

→ system is nonlinear

→ conventional circuit analysis techniques do not work

→ closed form solution is not possible

→ However, an iterative solution can be found

Lets examine the capacitive example

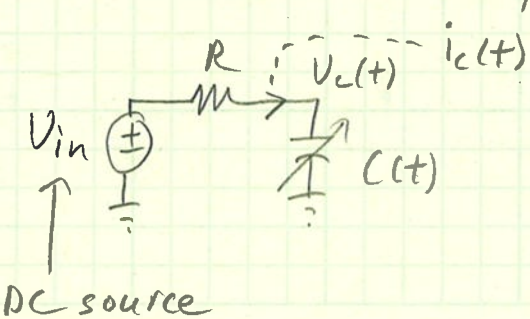

$$\therefore i_c(t) = \frac{V_{in} - V_c(t)}{R} = \dot{V}_c(t)\,C(t) + V_c(t)\,\dot{C}(t) \quad ①$$

Lets assume that $C(t) = C_0 + C_1(t)$ ②, where $C(t) > 0$ always

where $C_0$ is time-invariant

$C_1(t)$ is time-variant

$\therefore \dot{C}(t) = \dot{C}_1(t)$ ③

First, analyze the circuit as a linear time-invariant circuit with $C(t) = C_0$ and obtain the steady state value for $V_c(t)$, denoted $V_{c0}(t)$

Second, use $V_{c0}(t)$ with ① to find $i_{c1}(t)$

Third, use small signal analysis with $R$ to find $V_{c1}(t)$ in terms of $i_{c1}(t)$:

$$V_{ck}(t) = -i_{ck}(t)\,R \quad ④$$

Fourth, the next $i_c(t)$ term is found using

$$i_{c(k+1)}(t) = \dot{V}_{ck}(t)\,C(t) + V_{ck}(t)\,\dot{C}(t) \quad ⑤$$

Then, using ④ and ⑤:

$$V_c(t) = V_{c0}(t) + \sum_{k=1}^{\infty} \left[\dot{V}_{ck}(t)\,C(t) + V_{ck}(t)\,\dot{C}(t)\right] R^k$$

and

$$i_c(t) = \sum_{k=1}^{\infty} \left[\dot{V}_{ck}(t)\,C(t) + V_{ck}(t)\,\dot{C}(t)\right]$$

→ use as many terms as needed to achelve desired accuracy

→ Show example from my IET paper

# Nonlinear circuit analysis for time-variant microelectromechanical system capacitor systems

*Robert N. Dean, Christopher G. Wilson*

*Department of Electrical and Computer Engineering, Auburn University, Auburn, AL 36849, USA*
*E-mail: deanron@auburn.edu*

Published in Micro & Nano Letters; Received on 29th April 2013; Revised on 21st June 2013; Accepted on 2nd July 2013

Electrostatic transducers, consisting of time-variant capacitors, are utilised in many types of microelectromechanical system (MEMS) devices. Linear circuit theory is based on the premise of time-invariant passive devices. Time-variant capacitors generally result in one or more nonlinear differential equations that must be solved to obtain expressions for the voltage across or the current through the capacitor. An iterative approach can be used to provide an approximate solution to the nonlinear differential equation model of the Thévenin equivalent RC circuit. This solution technique is verified through comparison with a MATLAB Simulink® simulation of a MEMS capacitor that sinusoidally varies with time because of external stimuli.

**1. Introduction:** Time-variant capacitors are an integral part of many microelectromechanical system (MEMS) and nanodevices as both electrostatic actuators and as sensing structures. The primary electrostatic actuators are the parallel plate actuator (PPA) [1] and the comb drive actuator (CDA) [2]. These types of actuators are readily used in complex MEMS devices such as force-feedback accelerometers [3], gyroscopes [4], tunable RF devices [5] and microoptical devices [6]. As a detection mechanism, variable capacitors are used in applications such as inertial sensors [7], pressure sensors [8] moisture content sensors [9] and humidity sensors [10]. In each of these applications, the resulting capacitance is a function of a measurand, an external stimulus or an internal displacement, all of which can be modelled as a function of time. For a time-variant capacitor, the equation that relates current through it, $i_c(t)$, and voltage across it, $V_c(t)$ is

$$i_c(t) = \dot{V}_c(t)C(t) + V_c(t)\dot{C}(t) \tag{1}$$

In many applications, (1) is simplified by either using a DC voltage for $V_c(t)$ [11] or by making $V_c(t)$ an AC voltage where its frequency is so much higher than the bandwidth of $C(t)$ that $C(t)$ can reasonably be viewed as being time invariant [12]. However, this simplification is not appropriate for many applications. A common example is when a resistor is added between the time-variant MEMS capacitor and the voltage source, as shown in Fig. 1. This configuration is often used to protect the MEMS capacitive element and the voltage source in the event that the capacitor's electrodes make physical contact and electrically short [13]. Additionally, the circuit model in Fig. 1 could be the

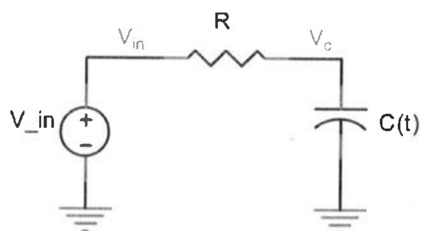


**Figure 1** *Schematic diagram of a time-variant capacitor in series with a resistor*

Thévenin equivalent circuit for a more complex circuit connected to $C(t)$.

The circuit is described by the differential equation

$$i_c(t) = \frac{V_{\text{in}} - V_c(t)}{R} = \dot{V}_c(t)C(t) + V_c(t)\dot{C}(t) \tag{2}$$

This equation is a first-order nonlinear ordinary differential equation, and it is therefore difficult to obtain a closed-form solution [14].

**2. Technique:** However, an iterative approach [15] can be used to obtain an approximate solution for this differential equation that yields functions for $i_c(t)$ and $V_c(t)$. In order to obtain an approximate solution, the capacitance needs to be modelled as

$$C(t) = C_0 + C_1(t) \tag{3}$$

where

$$\dot{C}(t) = \dot{C}_1(t) \tag{4}$$

where $C_0$ is defined as the time-invariant capacitance. $C_1(t)$ is the time-variant capacitance that must be smaller in magnitude than $C_0$, such that $C(t) > 0$. The circuit is first analysed as a linear circuit with a time-invariant capacitor equal to $C_0$ to obtain the steady-state solution for $V_c(t)$, denoted by $V_{c0}(t)$. An expression for $i_{c1}(t)$ is then found using $V_{c0}(t)$ with (2)–(4). The next step is to use a small-signal analysis with $R$ to find an expression for $V_{c1}(t)$ in terms of $i_{c1}(t)$ where

$$V_{ck}(t) = -i_{ck}(t)R \tag{5}$$

Then the next $i_c(t)$ term is found using

$$i_{c(k+1)}(t) = \dot{V}_{ck}(t)C(t) + V_{ck}(t)\dot{C}(t) \tag{6}$$

Equations (5) and (6) are then used to calculate as many terms as desired where

$$V_c(t) = V_{c0}(t) + \sum_{k=1}^{\infty} \left[\dot{V}_{ck}(t)C(t) + V_{ck}(t)\dot{C}(t)\right]R^k \tag{7}$$

and

$$i_c(t) = \sum_{k=1}^{\infty} \left[\dot{V}_{ck}(t)C(t) + V_{ck}(t)\dot{C}(t)\right] \quad (8)$$

**3. Verification:** For verification, consider the two primary types of micromachined capacitor structures, variable area overlap and variable gap. The model for a variable area overlap capacitor is

$$C(x) = \frac{\varepsilon_o \varepsilon_r w(x_o + x)}{d_o} \quad (9)$$

Since most MEMS devices are highly underdamped [16], they sinusoidally ring at their resonant frequency, $\omega_n$, whereas experiencing external stimuli, such as vibrational [17] or acoustic energy [18]. Therefore $x$ can be replaced by $\sin(\omega t)$ so that

$$C(t) = \frac{\varepsilon_o \varepsilon_r w(x_0 + x_1 \sin(\omega t))}{d_0} \quad (10)$$

where $x_1 < x_0$. For the special case where the area overlap capacitor consists of two interdigitated combs, $C(t)$ becomes

$$C(t) = \frac{n\beta \varepsilon_o \varepsilon_r w(x_0 + x_1 \sin(\omega t))}{d_0} \quad (11)$$

where $n$ is the number of interdigitated tooth pairs and $\beta$ is the fringing field correction factor. So, this capacitor can be modelled as

$$C(t) = y_1 + y_2 \sin(\omega t) \quad (12)$$

where

$$y_1 = \frac{n\beta \varepsilon_o \varepsilon_r w x_0}{d_0} \quad (13)$$

and

$$y_2 = \frac{n\beta \varepsilon_o \varepsilon_r w x_1}{d_0} \quad (14)$$

A variable gap MEMS capacitor has the model

$$C(t) = \frac{\varepsilon_o \varepsilon_r A}{x_0 + x_1 \sin(\omega t)} \quad (15)$$

For the case where $x_1 \ll x_0$, $C(t)$ can be approximated by

$$C(t) \simeq y_1 + y_2 \sin(\omega t) \quad (16)$$

where

$$y_1 = \frac{\varepsilon_o \varepsilon_r A}{x_0 - 0.5((x_1^2)/(x_0))} \quad (17)$$

and

$$y_2 = -y_1 \frac{x_1}{x_0} \quad (18)$$

Therefore both types of MEMS time-variant capacitors can be modelled by (3).

Consider the case where $V_{\text{in}}$ is a DC voltage source with a voltage of $V_{\text{DC}}$ that is less than the pull-in voltage in the case of a PPA [19] or the lateral instability voltage for a CDA [20]. $C(t)$ then becomes

$$C(t) = C_0 + C_1 \sin(\omega t) \quad (19)$$

where $C_1 < C_0$, and

$$\dot{C}(t) = C_1 \omega \cos(\omega t) \quad (20)$$

Using the circuit model in Fig. 1, $V_{c0} = V_{\text{DC}}$. Therefore from (6)

$$i_{c1}(t) = C(t)\dot{V}_{c0} + V_{c0}\dot{C}(t) = V_{\text{DC}} C_1 \omega \cos(\omega t) \quad (21)$$

and, using small signal analysis and (5)

$$V_{C1}(t) = -i_{c1}R = -RV_{\text{DC}} C_1 \omega \cos(\omega t) \quad (22)$$

Likewise, $V_{C1}(t)$ is used to find $i_{c2}(t)$ and $V_{C2}(t)$.

$$\dot{V}_{C1}(t) = RV_{\text{DC}} C_1 \omega^2 \sin(\omega t) \quad (23)$$

and

$$\begin{aligned} i_{c2} &= C(t)\dot{V}_{C1}(t) + V_{C1}(t)\dot{C}(t) \\ &= (C_0 + C_1 \sin(\omega t))(RV_{\text{DC}} C_1 \omega^2 \sin(\omega t)) \\ &\quad + (C_1 \omega \cos(\omega t))(-RV_{\text{DC}} C_1 \omega \cos(\omega t)) \end{aligned} \quad (24)$$

which simplifies to

$$i_{c2}(t) = C_0 RV_{\text{DC}} C_1 \omega^2 \sin(\omega t) - C_1^2 \omega^2 RV_{\text{DC}} (\cos^2(\omega t) - \sin^2(\omega t)) \quad (25)$$

and finally to

$$i_{c2}(t) = C_0 RV_{\text{DC}} C_1 \omega^2 \sin(\omega t) - C_1^2 \omega^2 RV_{\text{DC}} \cos(2\omega t) \quad (26)$$

Then,

$$\begin{aligned} V_{c2}(t) &= -Ri_{c2}(t) = -C_0 R^2 V_{\text{DC}} C_1 \omega^2 \sin(\omega t) \\ &\quad + C_1^2 \omega^2 R^2 V_{\text{DC}} \cos(2\omega t) \end{aligned} \quad (27)$$

and

$$\begin{aligned} \dot{V}_{c2}(t) &= -C_0 R^2 V_{\text{DC}} C_1 \omega^3 \cos(\omega t) \\ &\quad - 2C_1^2 \omega^3 R^2 V_{\text{DC}} \sin(2\omega t) \end{aligned} \quad (28)$$

Next $i_{c3}$(t) and $V_{c3}$(t) are calculated

$$\begin{aligned} i_{c3}(t) &= C(t)\dot{V}_{C2}(t) + V_{C2}(t)\dot{C}(t) \\ &= (C_0 + C_1 \sin(\omega t))(-C_0 R^2 V_{\text{DC}} C_1 \omega^3 \cos(\omega t) \\ &\quad - 2C_1^2 \omega^3 R^2 V_{\text{DC}} \sin(2\omega t)) \\ &\quad + (C_1 \omega \cos(\omega t))(-C_0 R^2 V_{\text{DC}} C_1 \omega^2 \sin(\omega t) \\ &\quad + C_1^2 \omega^2 R^2 V_{\text{DC}} \cos(2\omega t)) \end{aligned} \quad (29)$$

By rearranging terms

$$\begin{aligned} i_{c3}(t) &= -C_0^2 R^2 V_{\text{DC}} C_1 \omega^3 \cos(\omega t) \\ &\quad - 2C_0 C_1^2 \omega^3 R^2 V_{\text{DC}} \sin(2\omega t)) \\ &\quad - C_0 R^2 V_{\text{DC}} C_1^2 \omega^3 \sin(\omega t)\cos(\omega t) \\ &\quad - 2C_1^3 \omega^3 R^2 V_{\text{DC}} \sin(\omega t)\sin(2\omega t) \\ &\quad - C_0 R^2 V_{\text{DC}} C_1^2 \omega^3 \sin(\omega t)\cos(\omega t) \\ &\quad + C_1^3 \omega^3 R^2 V_{\text{DC}} \cos(\omega t)\cos(2\omega t) \end{aligned} \quad (30)$$

Utilising trigonometric identities

$$\sin(\omega t)\cos(\omega t) = 0.5\sin(2\omega t) \quad (31)$$

$$\sin(\omega t)\sin(2\omega t) = 0.5(\cos(\omega t) - \cos(3\omega t)) \quad (32)$$

$$\cos(\omega t)\cos(2\omega t) = 0.5(\cos(\omega t) + \cos(3\omega t)) \quad (33)$$



*Micro & Nano Letters*, 2013, Vol. 8, Iss. 9, pp. 515–518
doi: 10.1049/mnl.2013.0239

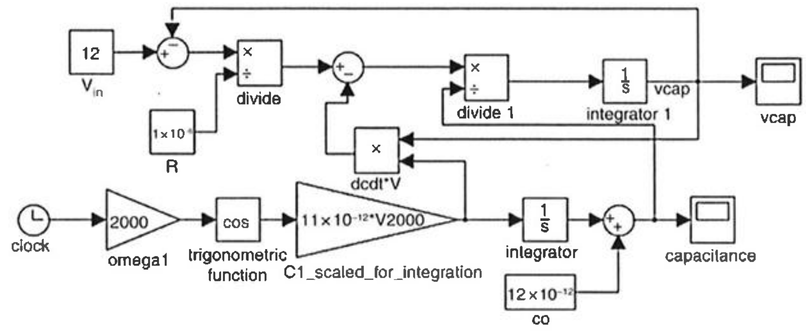


**Figure 2** *MATLAB Simulink® model*

Equation (30) now can be rewritten as

$$\begin{aligned} i_{c3}(t) = & -C_0^2R^2V_{\mathrm{DC}}C_1\omega^3\cos(\omega t) \\ & - 2C_0C_1^2\omega^3R^2V_{\mathrm{DC}}\sin(2\omega t)) \\ & - C_0R^2V_{\mathrm{DC}}C_1^2\omega^3\sin(2\omega t) \\ & - C_1^3\omega^3R^2V_{\mathrm{DC}}(\cos(\omega t) - \cos(3\omega t)) \\ & + 0.5C_1^3\omega^3R^2V_{\mathrm{DC}}(\cos(\omega t) + \cos(3\omega t)) \end{aligned} \tag{34}$$

which reduces to

$$\begin{aligned} i_{c3} = & -C_0^2R^2V_{\mathrm{DC}}C_1\omega^3\cos(\omega t) - 3C_0C_1^2\omega^3R^2V_{\mathrm{DC}}\sin(2\omega t) \\ & - C_1^3\omega^3R^2V_{\mathrm{DC}}(0.5\cos(\omega t) - 1.5\cos(3\omega t)) \end{aligned} \tag{35}$$

Finally, the third iteration voltage $V_{c3}(t)$ can be found using (35) in (5)

$$V_{c3}(t) = -Ri_{c3}(t) \tag{36}$$

or

$$\begin{aligned} V_{c3} = & +C_0^2R^3V_{\mathrm{DC}}C_1\omega^3\cos(\omega t) + 3C_0C_1^2\omega^3R^3V_{\mathrm{DC}}\sin(2\omega t) \\ & + C_1^3\omega^3R^3V_{\mathrm{DC}}(0.5\cos(\omega t) + 1.5\cos(3\omega t)) \end{aligned} \tag{37}$$

Observe that $V_{c0}$ is a DC term. $V_{C1}(t)$ is an AC term proportional to $RC_1\omega$. $V_{C2}(t)$ possesses AC terms proportional to $R^2(C_1)^2\omega^2$ and $R^2C_1C_0\omega^2$. $V_{C3}(t)$ contains AC terms proportional to $R^3(\text{capacitance})^3\omega^3$.

MATLAB Simulink® was used to solve (2) numerically where the capacitor was modelled by (19) with values for $C_0$ and $C_1$ of 12 and 11 pF, respectively, for a $V_{in}$ of 12 V and an $R$ of 1 MΩ. A value of 2000 rad/s was used for $\omega$. The Simulink numerical solver was set to fixed-step ODE3 (Bogacki-Shampine) with a fixed-step size of $1\times10^{-9}$ s. The Simulink model is presented in Fig. 2.

One period of simulation data are presented in Fig. 3 along with the first four terms for the example, $V_{c0}$ and terms from (22), (27) and (37). The error terms, that is, the Simulink solution minus the iterative solution terms, are presented in Fig. 4, demonstrating

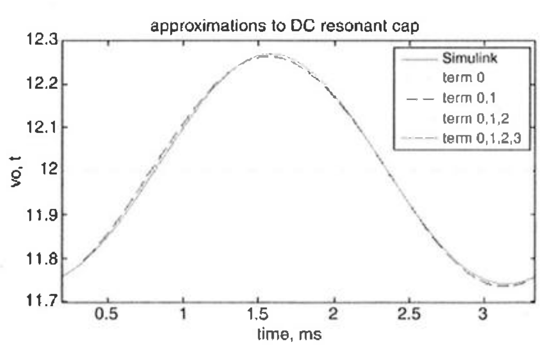


**Figure 3** *Simulink® results with successive terms added*

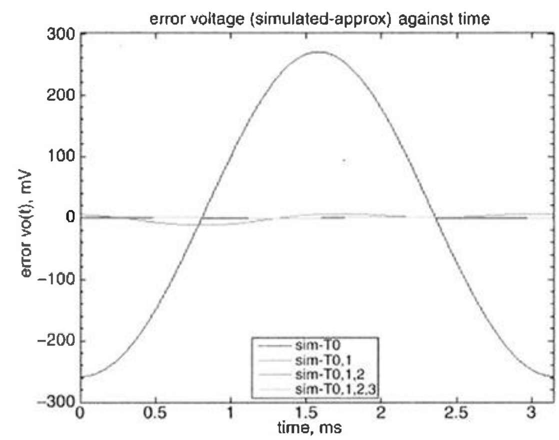


**Figure 4** *Graph of the error between the Simulink® solution and the iterative solution*

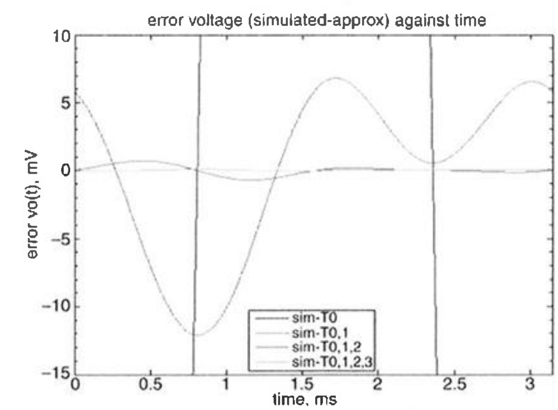


**Figure 5** *Graph of the error between the Simulink® solution and the iterative solution zoomed in on the higher-order terms*

that the error decreases when each successive term is included in the approximate solution. Fig. 5 zooms in on the higher-order error terms for clarity. The DC $V_{c0}$ error term has an error voltage exceeding 200 mV, whereas the inclusion of the first through fourth-order terms drops the error voltage to $< 1$ mV.

**4. Conclusions:** Linear circuit analysis is based on the premise of time-invariant passive devices. Many MEMS sensors and actuators utilise time-variant capacitors for sensing and/or actuation. When the voltage across the capacitor is not a constant and the circuit can be modelled as a Thévenin equivalent circuit, with a DC or a constant amplitude sinusoidal voltage source, the circuit equation becomes a nonlinear ordinary differential equation. An approximate solution technique for solving this equation has been presented and compared with a numerical solution using MATLAB Simulink®. For many applications, this technique affords a reasonably simple method for performing circuit analysis on typical interface circuits utilised with MEMS time-variant capacitive elements.

## 5 References


[1] Dong L., Edwards J.: 'Closed-loop voltage control of a parallel-plate MEMS electrostatic actuator'. Proc. 2010 American Control Conf., Baltimore, MD, USA, 2010, pp. 3409–3414

[2] Wooldridge J., Muniz-Piniella A., Stewart M., Shean T.A.V., Weaver P.M.: 'Vertical comb drive actuator for the measurement of piezoelectric coefficients in small-scale systems', *J. Micromech. Microeng.*, 2013, **23**, p. 12

[3] Meng Z., Jingqing H., Tingting Z., *ET AL.*: 'Research on nonlinearity of closed-loop capacitive accelerometer resulting from time-division force feedback'. Proc. IEEE 2012 Electron Devices and Solid State Circuits, Bangkok, Thailand, 2012, p. 4

[4] Hudson T.D., Holt S.W., Ruffin P., *ET AL.*: 'High-performance microfabricated angular rate sensor', *J. Microlithogr. Microfabr. Microsyst.*, 2005, **4**, (4), p. 8

[5] Sundaram A., Maddela M., Ramadoss R., Feldner L.M.: 'MEMS-base electronically steerable antenna array fabricated using PCB technology', *J. Microelectromech. Syst.*, 2008, **17**, pp. 356–362

[6] Zhang J., Zhang Z., Lee Y.C., Bright V.M., Neff J.: 'Design and invention of multi-level digitally positioned micromirror for open-loop controlled applications', *Sens. Actuators A, Phys.*, 2003, **103**, pp. 271–283

[7] Xie H., Fedder G.K.: 'A DRIE CMOS-MEMS gyroscope'. Proc. IEEE Sensors, Orlando, FL, USA, 2002, pp. 1413–1418

[8] Ridzuan N.A.A., Masuda S., Miki N.: 'Flexible capacitive sensor encapsulating liquids as dielectric with a largely deformable polymer membrane', *Micro Nano Lett.*, 2012, **7**, pp. 1193–1196

[9] Dean R.N., Rane A., Baginski M., Richard J., Hartzog Z., Elton D.J.: 'A capacitive fringing field sensor design for moisture measurement based on printed circuit board technology', *IEEE Trans. Instrum. Meas.*, 2012, **61**, pp. 1105–1112

[10] Li J., Liu Y., Tang M., Li J., Lin X.: 'Capacitive humidity sensor with a coplanar electrode structure on anodized porous alumina film', *Micro Nano Lett.*, 2012, **7**, pp. 1097–1100

[11] Dean R., Flowers G., Horvath R., *ET AL.*: 'Characterization and experimental verification of the nonlinear distortion in a technique for measuring relative velocity between micromachined structures in normal translational motion', *IEEE Sens. J.*, 2007, **7**, pp. 496–501

[12] Senturia S.D.: 'Microsystem design' (Springer, New York, 2001), pp. 502–504

[13] De Coster J., Rottenberg X., Sangameswaran S., Ekkels P., Tilmans H.A.C., De Wolf I.: 'Robustness of electrostatic MEMS actuators against electrical overstress'. Proc. Transducers 2009, Denver, CO, USA, 2009, pp. 893–896

[14] DuChateau P.: 'First order nonlinear equations', available at http://www.math.colostate.edu/~pauld/M345/1stOrderNLODE.pdf, accessed 24 April 2013

[15] Li Y.: 'Monotone iterative method for numerical solution of nonlinear ODEs in MOSFET RF circuit simulation', *Math. Comput. Model.*, 2012, **51**, pp. 320–328

[16] Yasumura K.Y., Stowe T.D., Chow E.M., *ET AL.*: 'Quality factors in micron- and submicron-thick cantilevers', *J. Microelectromech. Syst.*, 2000, **9**, pp. 117–125

[17] Brown T.G.: 'Harsh military environments and microelectromechanical (MEMS) devices'. Proc. 2003 IEEE Sensors, Toronto, Canada, 2003, pp. 753–760

[18] Weinberg M.S., Kourepenis A.: 'Error sources in in-plane silicon tuning-fork MEMS gyroscopes', *J. Microelectromech. Syst.*, 2006, **15**, (3), pp. 479–491

[19] Dean R.N., Wilson C., Brunsch J.P., Hung J.Y.: 'A synthetic voltage division controller to extend the stable operating range of parallel plate actuators'. Proc. 2011 IEEE Multi-Conf. Systems and Control, Denver, CO, USA, 2011, pp. 1068–1074

[20] Borovic B., Lewis F.L., Liu A.Q., Kolesar E.S., Popa D.: 'The lateral instability problem in electrostatic comb drive actuators "modeling and feedback control" ', *J. Micromech. Microeng.*, 2006, **16**, pp. 1233–1241





doi: 10.1049/mnl.2013.0239